Chapter 4

FMR Measurements of Magnetic Nanostructures

Manish Sharma, Sachin Pathak and Monika Sharma

Additional information is available at the end of the chapter

http://dx.doi.org/10.5772/56615

1. Introduction

Ferromagnetic nanowires showed solitary and tunable magnetization properties due to their inherent shape anisotropy. The fabrication of such nanowires in polycarbonate track-etched and anodic alumina membranes have been widely studied during the last 15 years [1-2]. Their potential applications might be explored in spintronic devices and more specifically in magnetic random access memory (MRAM) and magnetic logic devices [3-5]. Furthermore, microwave devices, such as circulators or filters for wireless communication and automotive systems can be fabricated on ferromagnetic nanowires embedded in AAO substrates [6-9].

This chapter begins with a brief overview of the historical development of the theory of ferromagnetic resonance in magnetic nanostructures. State-of-the-art calculations for resonance frequency in ferromagnetic nanowires (solid and hollow) and multilayer nanowires are presented. In addition, experimental approach to synthesis such structures and detecting material properties using various techniques will be discussed in brief. Recently, due to the development of spintronics, there have been increasing interests in the microwave dynamics of one-dimensional structures such as nanowires and two dimensional structures like multilayer magnetic films. The most important parameters that control dynamic behaviors are the internal fields and damping constant. The ferromagnetic nanowires in anodic alumina (AAO) templates seem to be attractive substrates for microwave applications. Since they have high aspect ratio, electromagnetic waves can easily penetrate through them. They exhibit ferromagnetic resonance (FMR) even at zero bias fields and, due to their high saturation magnetization, operating frequency can be tuned with DC fields.

FMR is a useful technique in the measurement of magnetic properties of ferromagnetic materials. It has been applied to a range of materials from bulk ferromagnetic materials to nano-scale magnetic thin films and now a day's people have started research to characterise nanoparticles and nanowires systems. The dynamic properties of magnetic materials can be easily perturbed by ferromagnetic resonance (FMR), as they can excite standing spin waves

due to magnetic pinning [10-11,31,32]. It also yields direct information about the uniform precession mode of the nanowires which can be related to the average anisotropy magnitude [12-15]. Several measurement techniques which have been used to characterise magnetization dynamics such as femtosecond spectroscopy [16-18], pulse inductive microwave magnetometer [19], FMR force microscopy [20], network analyzer FMR [21,31,32] and high-frequency electrical measurements of magnetodynamics [22]. All these techniques can be used for modern application for example in telecommunications and data storage systems.

In the present chapter, we deal with magnetic nanostructures such as nanowires and multilayered nanodiscs and rings which exhibit unique FMR responses since their various anisotropy energies are strongly influenced by size and shape [33]. In addition, interactions between multilayered segments can be tailored such that the FMR response is not only angle-dependent but also influenced strongly at certain frequencies [32]. In this chapter, we shall be describing three different aspects of this topic:

1. We first develop the theory of FMR response of densely packed nanowire arrays that can be treated as two-dimensional periodic nanostructures. We then extend the theory to three-dimensional structures, which can be made using multilayered nanowires.
2. We then describe how to synthesize such nanowire arrays and also direct measurements of such structures. Several different experimental techniques are discussed.
3. We then continue the treatment to describe the use of such periodic nanowire arrays in microwave devices to exhibit nonlinear responses and also for circulators and isolators. Although the effects seen till now are weak, these are still quite promising.

2. Fundamental theory of ferromagnetic resonance

Ferromagnetic resonance (FMR) is a very powerful experimental technique in the study of ferromagnetic nanomaterials. The precessional motion of a magnetization $\boldsymbol{M}$ of ferromagnetic material about the applied external magnetic field $\boldsymbol{H}$ is known as the Ferromagnetic resonance (FMR). In the physical process of resonance, the energy is absorbed from rf transverse magnetic field h_{rf}, which occurred when frequency matched with precessional frequency (ω). The precession frequency depends on the orientation of the material and the strength of the magnetic field. It allows us to measure all the most important parameters of the material: Curie temperature, total magnetic moment, relaxation mechanism, elementary excitations and others.

A single domain magnetic particle with ellipsoid shape was considered as in [Kittel] to drive the resonance condition for the phenomenon of ferromagnetic resonance. A uniform, static magnetic field H is applied along the z-axis and set the sample in a microwave cavity. A resonance is observed at a frequency given by

$$\hbar\omega = g\mu_B\sqrt{[H+(N_x-N_z)M][H+(N_y-N_z)M]}. \tag{1}$$

N_x, N_y, N_z are the demagnetization factors in the x, y, z directions, and so on, and where g is the spectroscopic splitting factor (Lande factor) and $\mu_B = e\hbar/2m_e$ is the Bohr magneton. The demagnetizing factors affect the shape anisotropy of the magnetic material depending upon its geometry to be ellipsoid, sphere, thin film etc.

Part of the classical approach to ferromagnetism is to replace the spins by a classical micro-spin vector $\boldsymbol{M}$ magnetization. The time-dependence of the magnetization can be obtained directly by calculating the torque acting on $\boldsymbol{M}$ by an effective field $\boldsymbol{H}_{eff}$,

$$\frac{d\boldsymbol{M}}{dt} = -\gamma \boldsymbol{M} \times \boldsymbol{H}, \tag{2}$$

where $\gamma = g\mu_b/\hbar$ is a gyromagnetic ratio. This equation represents an undamped precession of the magnetization. From experiments actual changes of the magnetization are known to decay in a finite time. The occurrence of a damping mechanism leads to reversal of the magnetization towards the direction of $\boldsymbol{H}$ within several nanoseconds. The damping is just added as a phenomenological term to Eq. 2.

$$\frac{d\boldsymbol{M}}{dt} = -\gamma \boldsymbol{M} \times \left(\boldsymbol{H}_{eff} - \frac{\alpha}{\gamma M_s} \frac{d\boldsymbol{M}}{dt} \right) = -\gamma \boldsymbol{M} \times \boldsymbol{H}_{eff} + \frac{\alpha}{M_S} \boldsymbol{M} \times \frac{d\boldsymbol{M}}{dt} \tag{3}$$

where α is the dimensionless Gilbert damping constant, of order 10^{-2} in ferromagnetic thin films. Eq. 3 is known as Landau-Lifshitz-Gilbert equation after Gilbert introduces the damping term. H_{eff} is the total effective magnetic field which is a sum of static applied magnetic field (H), dynamic magnetic field (h_{rf}) and internal magnetic field (H_{in}). Internal field constitutes various magnetic anisotropies such as magnetocrystalline anisotropy, shape anisotropy, and magnetoelastic anisotropy etc. This equation therefore describes torque acting on $\boldsymbol{M}$. This torque leads to a rotation of the magnetization towards the direction of the external magnetic field. The damping causes decay in precessional motion which by applying a dynamic magnetic field becomes continuous as shown in Fig. 1.

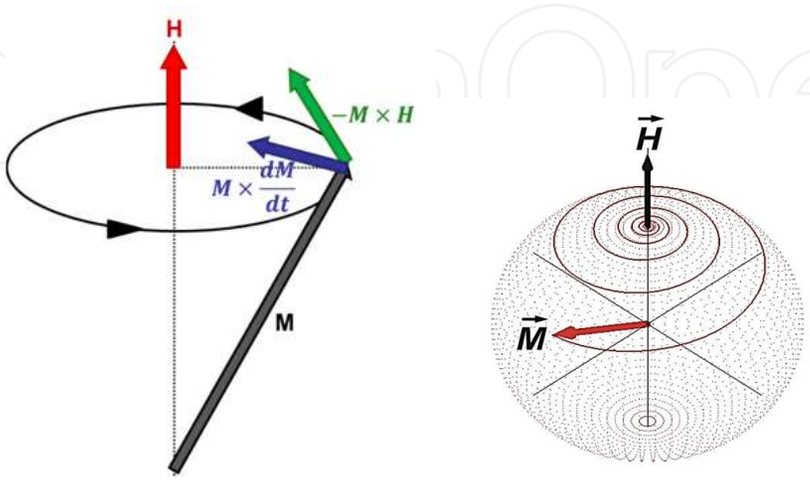

Figure 1. (a) Torque components exerted on the magnetization $\boldsymbol{M}$ by rotational field $\boldsymbol{H}$ (b) Motion of $\boldsymbol{M}$ for constant $\boldsymbol{H}$.

3. FMR dispersion relation for nanostructures

Due to miniaturization from bulk to the nanoscale, material properties shows a drastic change like surface-to-volume ratio, electron transport, thermodynamic fluctuations, defects etc. The nanomagnetic material demonstrates distinct magnetic response due to various anisotropies. The one-dimensional nanostructures such as nanowires, nanotubes, nanorods and nanorings are the area of recent research for data storage applications, sensors, biomedical drugs, microwave devices. To perturb the dynamic magnetization in these structures, ferromagnetic resonance is an effective tool.

In case of a system which incorporates an array of nanowires dipole-dipole interaction, shape anisotropy, crystalline anisotropy and Zeeman energy interaction plays a complex role. Therefore the total energy will be the sum of all internal energies.

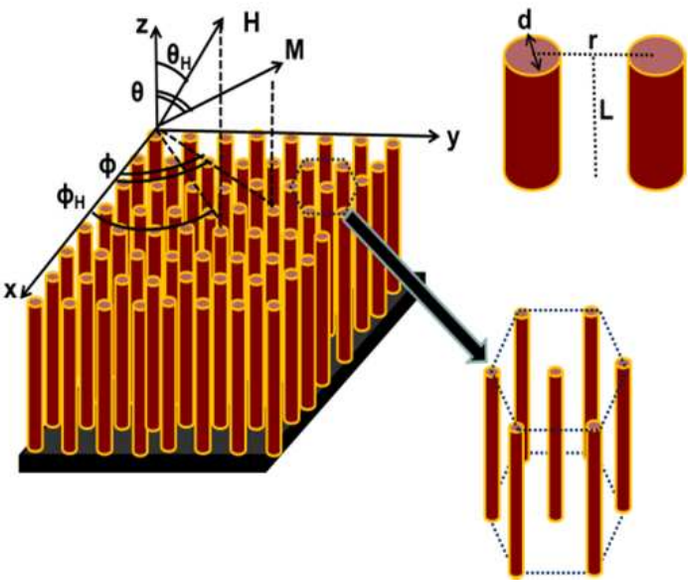

Figure 2. Coordinate system for an array of nanowires

Fig. 2 shows the schematic of an array of nanowires with relative orientation of the magnetization ***M*** and the applied magnetic field ***H*** *w.r.t* nanowire axis in spherical coordinate systems. The free energy density equation for an array of magnetic nanowires in the presence of external magnetic field at angles (θ_H) from nanowires axis can be written as

$$\mathrm{E} \approx -\mathrm{MH}\left(\sin\theta\sin\theta_H\cos\left(\phi-\phi_H\right)+\cos\theta\cos\theta_H\right)+K_{eff}\sin^2\theta \tag{4}$$

where K_{eff} is the effective uniaxial anisotropy which can be written as

$$\mathrm{K}_{eff} = \pi\mathrm{M}^2\left(1-3\mathrm{P}\right)+\mathrm{K}_U \tag{5}$$

The first term includes the dipole-dipole interaction between the nanowires and second term represents second-order uniaxial anisotropy along the wire axis. P is the porosity which can be obtained from

$$\mathrm{P} = \frac{\pi}{2\sqrt{3}} \frac{d^2}{r^2} \tag{6}$$

where d is the diameter of the pore and r is the centre-to-centre inter-wire distance between the pores. The equilibrium values for polar angles are obtained by minimizing the energy term

$$E_\theta = \frac{\partial E}{\partial \theta} = 0 \tag{7}$$

$$\mathrm{E}_\theta = -\mathrm{MH}\left(\cos\theta \sin\theta_H \cos\left(\phi - \phi_H\right) - \sin\theta \cos\theta_H\right) + K_{eff} \sin 2\theta = 0 \tag{8}$$

From eq (8) we retrieve the dispersion relation which can be written as

$$\left(\frac{\omega}{\gamma}\right)^2 = \left[\mathrm{H}\cos\left(\theta - \theta_\mathrm{H}\right) + \mathrm{H}_\mathrm{eff}\cos^2\theta\right]\left[\mathrm{H}\cos\left(\theta - \theta_\mathrm{H}\right) + \mathrm{H}_\mathrm{eff}\cos 2\theta\right] \tag{9}$$

Here, $\mathrm{H}_{eff} \approx 2\mathrm{K}_{eff} / \mathrm{M}_S$ is the effective anisotropy field that comes from a combination of effects including shape, magnetocrystalline and magnetoelastic anisotropy. Therefore from eq (5)

$$\mathrm{H}_{eff} = 2\pi M_S\left(1 - 3P\right) + 2\frac{K_U}{M_S} \tag{10}$$

For the case of multilayer nanowires, the effective anisotropy field H_{eff} is given by

$$\mathrm{H}_{eff} = 2\pi M_S\left(1 - 3\{1 - f(1 - P)\}\right) + 2\frac{K_U}{M_S} \tag{10a}$$

where, $f \approx \frac{h_m}{h_{nm} + h_m}$, h_m and h_{nm} represents magnetic and non-magnetic thicknesses in multilayer section. If h_{nm} = 0 (i.e. no non-magnetic spacer layer), the above equation represents the case of a single-element nanowire. Depending upon the direction of the external magnetic field along the easy axis of the nanowires, we can determine the various cases:

Case 1: H|| to the wire and $\mathrm{H}_{eff}>0$

$$\frac{\omega}{\gamma} = H + H_{eff} \tag{11}$$

Case 2: H|| to the wire and $\mathrm{H}_{eff}<0$

$$\frac{\omega}{\gamma} = H_{eff} - H \tag{12}$$

Case 3: $\mathrm{H}_\perp$ easy axis and $\mathrm{H}<\mathrm{H}_{eff}$

$$\left(\frac{\omega}{\gamma}\right)^2 = \left(H^2{}_{eff} - H^2\right) \tag{13}$$

Case 4: $H_{\perp}$ easy axis, $H>H_{eff}>0$

$$\left(\frac{\omega}{\gamma}\right)^2 = H(H - H_{eff}) \tag{14}$$

The frequency-field characteristics can be studied from these relations for various cases of the direction of the applied field and corresponding angular variation with resonance field of the nanowires as shown in Fig. 3. The horizontal line shows the intersection of the dispersion relation and indicates where in an FMR spectrum the resonance lines would be found for a fixed frequency in Fig. 3(a).

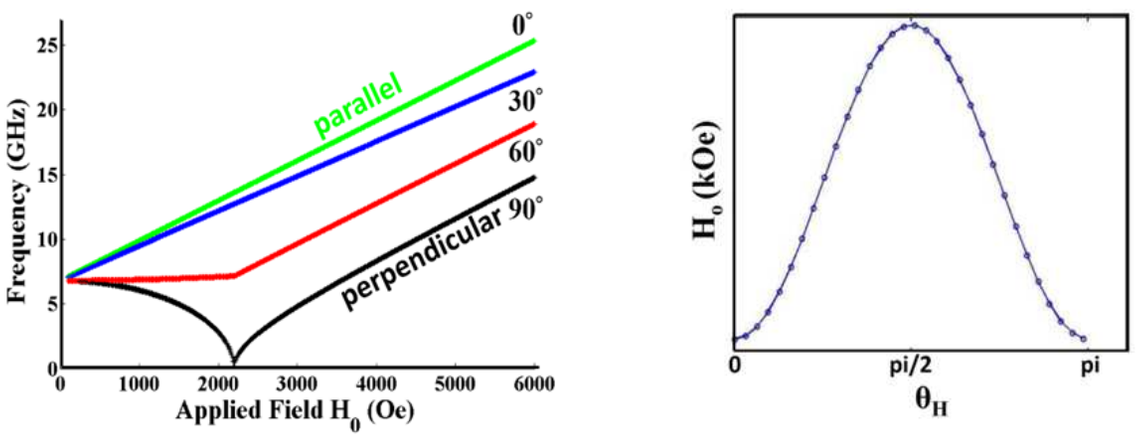

a b

Figure 3. Simulated plots (a) dispersion relation for Ni nanowires for various angles in which the external magnetic field is applied (b) resonance field as a function of the externally applied field angle θ_H.

4. Sample preparation and characterization

During last decade magnetic nanowires have attracted enormous research attention in many areas of advanced nanotechnology, including patterned magnetic recording media, materials for optical and microwave applications. Template assisted growth of nanostructures under constant potential in several electrolytes has been carried out by researchers for over 30 years. In comparison to other deposition techniques (sputtering and MBE) electrodeposition is a low cost and simple technique to fabricate magnetic nanowires and multilayers. Arrays of Co nanowires were fabricated by template assisted electrochemical deposition into the nanometer-sized pores.

5. Growth of nanostructures

Templates

Nanowires were grown by using two different types of templates (commercially available) polycarbonate track etched (PCTE) and aluminum oxide (AAO) from Whatman. These templates are completely different from each other due to their qualities as well as the preparation methods. The methods used for fabrication and properties of templates are given below;

Polycarbonate track etched (PCTE)

In PCTE template, the pore size varies from 20nm to 200nm and the thickness of ~6μm. To fabricate the PCTE template, initially high energy particle are used to bombard it to produce the path. Later these paths are etched in different chemical bath. The size of the pores is determined by the etching process. Fig.4(a) shows a SEM picture of a commercial PCTE membrane, with a reported pore size of 100 nm. Although the pores seem to have similar diameters, the pore placement is random. The pores density is quite low (in the range of 10^{10} to 10^{12} per cm^2) in case of PCTE.

Anodic aluminum oxide (AAO)

In 1995, Masuda and Fukuda reported the method to fabricate highly ordered nanohole arrays on aluminum foil. Double anodization of aluminium in acidic solution is adopted to fabricate porous alumina template. The beauty of these templates is their cylindrical pores of uniform diameter, arranged in hexagonal arrays with a thin oxide layer exist at the bottom. Anodic Aluminum Oxide (AAO) templates have been successfully used as templates for the growth of nanowires by electrodeposition. In order to fabricate the AAO template the aluminum is cleaned in the acidic medium to remove the surface impurities. Further the cleaned aluminium processed by two step anodization described by Masuda. The pore size and spacing between pore in the alumina templates are controlled by the anodization voltage.

Temperature of electrolyte also plays a important role in pore parameters. The pores in AAO template cylindrical and highly dense which makes it a good candidate to study the interaction effect between the nanowires on magnetic properties. Fig. 4(b)-(c) shows the SEM micrograph of AAO templates.

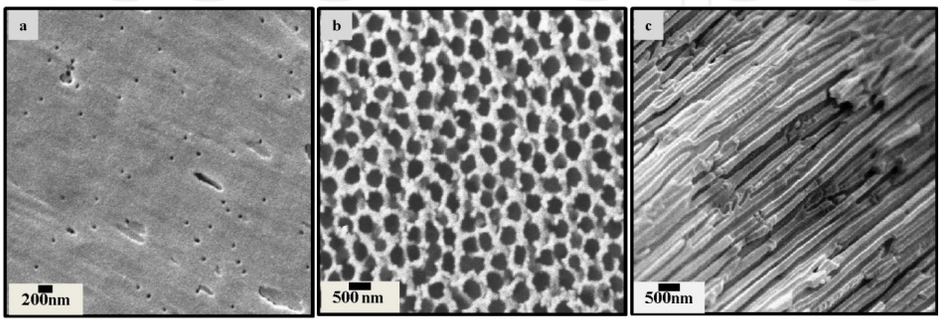

Figure 4. SEM micrograph of membranes (a) Polycarbonate (b) Anodic alumina (Top view) and (c) anodic alumina (cross-section view).

Template assisted electrodeposition technique

Electrodeposition process involves the electric current to reduce cations from electrolyte and deposited that material as a thin film onto a conducting substrate. At the cathode the metal reduction takes place and metal deposits according to:

$$\mathbf{Mn^{+} + n\ e^{-} = M(s)}$$

In order to form the nanowires, the cations from electrolyte move through the non-conducting template (AAO/ PCTE) having nanosized pores and deposited on the conducting substrate.

The desired material properties depends upon the various process parameters like electrolyte composition, bath pH, mode of deposition (DC, pulse and AC) and deposition temperature.

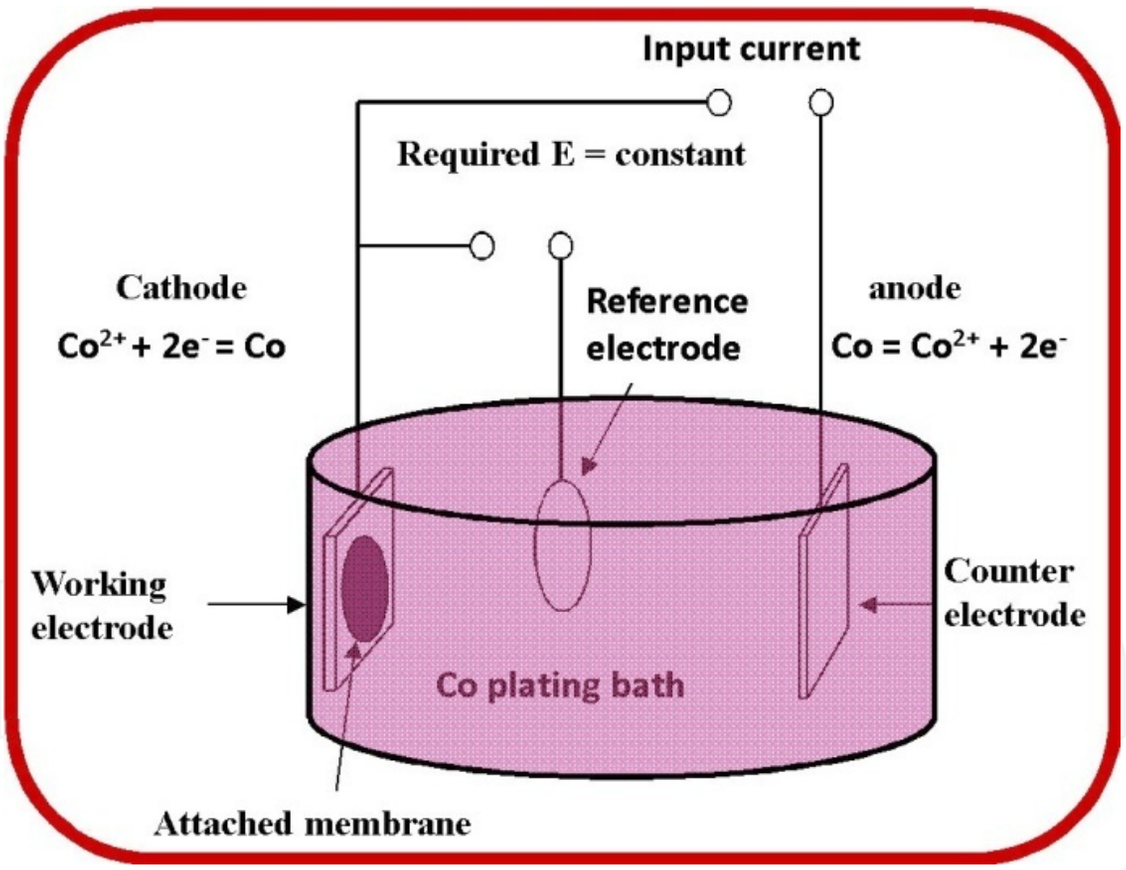

Figure 5. Schematic representation of three-electrode electrochemical cell setup employed. AAO template mounted electrodes act as a working electrodes (WE), platinum foil counter electrode (CE) and Saturated calomel electrode (SCE), reference electrode (RE).

Fig.5 illustrates the three-electrode cell set-up used in this study. A platinum foil and a saturated calomel electrode (SCE) were used as the anode (or counter electrode) and as a reference electrode respectively. The steps of preparation of nanostructure are as followed;

Steps involved in the template assisted synthesis of nanowires

Step 1: The porous anodic alumina (AAO) /polycarbonate templates were taken and one side of the AAO were sputtered with Au by RF sputtering, which acted as the working electrode in a three-electrode electrochemical cell.

Step 2: The electrodeposition solution was restrained to the other side of the membrane so that deposition was initiated onto the Au layer within the pores. The array of Co nanowires was deposited from a solution of 25 gm/L $CoSO_4.7H_2O$, 5 gm/L H_3BO_3 and sodium Lauryl Sulphate (SLS), which is used to reduce the surface tension of water for proper wetting of pores.

Step 3: The cyclic voltammetry is used to figure out the constant deposition potential of the working electrode with respect to a standard reference electrode **RE** to get the favourable condition for deposition.

Step 4: The growth of nanowires is carried at the optimized potential.

Step 5: For further investigation of freely standing nanowires, the templates is used to dissolve in an appropriate solution. Etching solution for AAO and PCTE are sodium hydroxide and dichloromethane respectively.

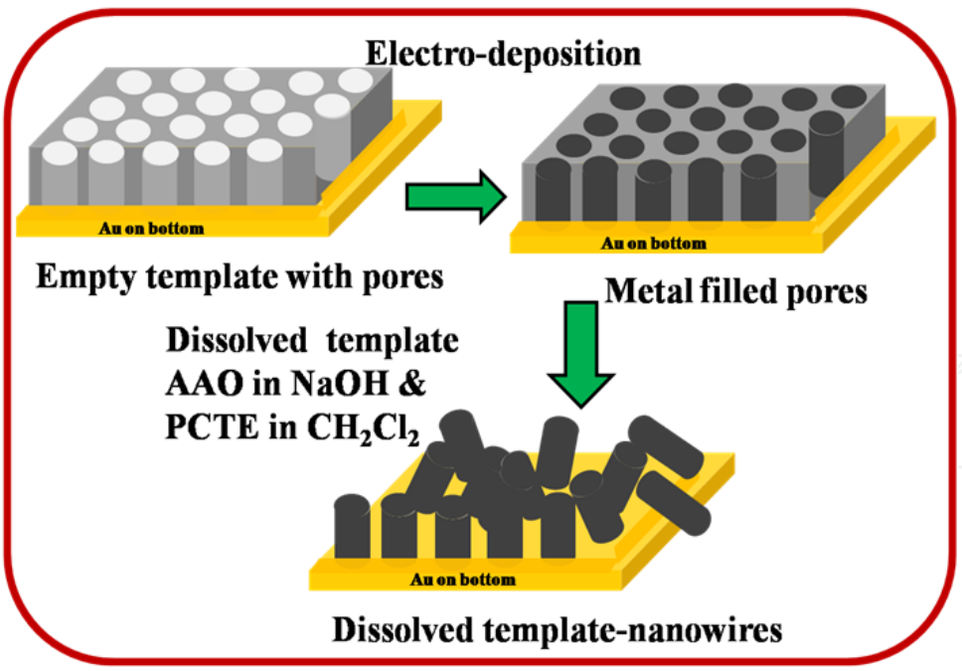

Figure 6. Schematic illustration of the growth of magnetic nanowire in alumina template by electrodeposition process.

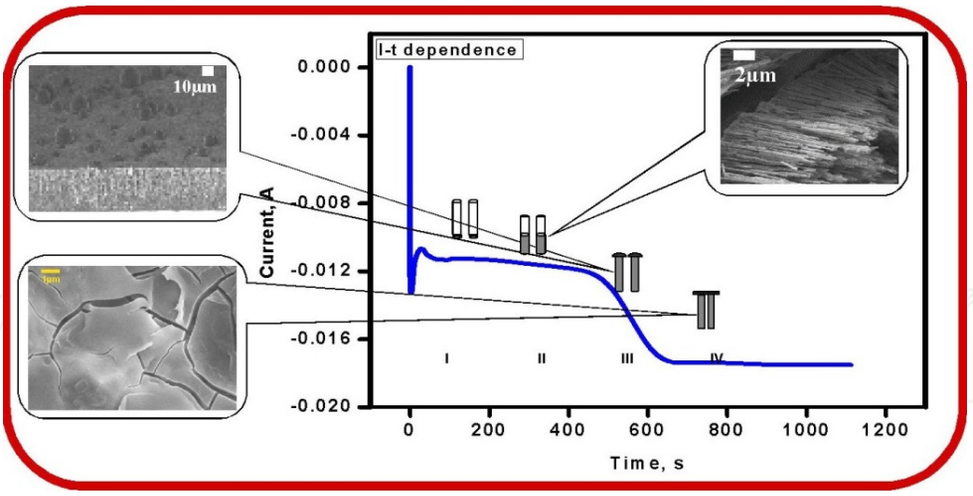

Figure 7. Typical choronoamperometery plot during potentiostatic electrodeposition taken during the fabrication of Co nanowires. The various stage of pore filling during deposition is shown as insets at the respective current-time positions.

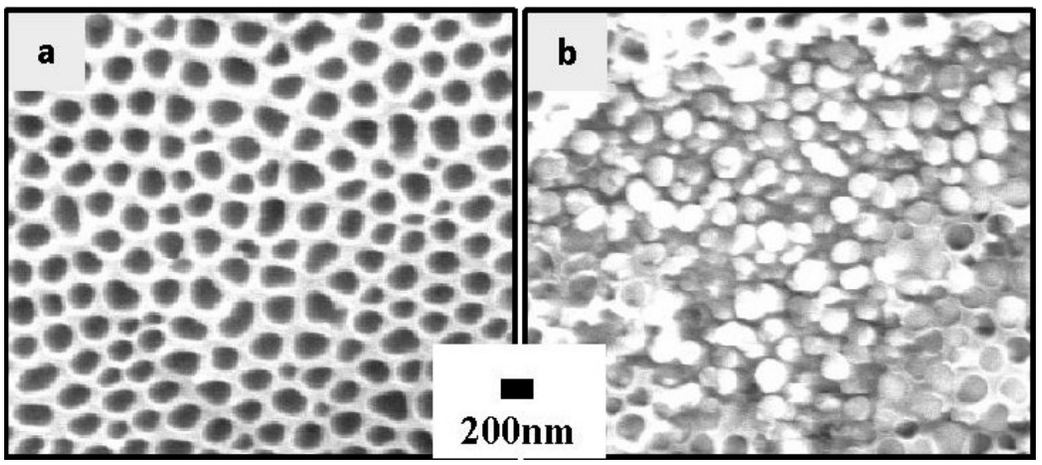

Figure 8. Scanning electron micrograph (SEM) of empty and filled surface morphology of the template.

6. Characterization of nanostructures

Scanning electron microscopy

For scanning electron microscopy (SEM), the template containing nanowires is partially released from their template by appropriate solution. To remove the residual part of template the etched sample is cleaned by deionised water. To carry out the surface analysis secondary electron imaging in scanning electron microscope has been utilized. Surface morphology of Co nanowire was investigated by scanning electron microscope (SEM: ZEISS EVO 50) operating at 20 kV accelerating voltage by secondary electron imaging. Fig. 8 shows the SEM micrograph of empty AAO and filled with nanowires. The morphology of grown nanowires in PCTE template can be clearly seen in Fig. 9(a). Side and top view of AAO assisted nanowires are presented in Fig. 9(b & c). The growth density of nanowires in AAO template is more as compared to PCTE template.

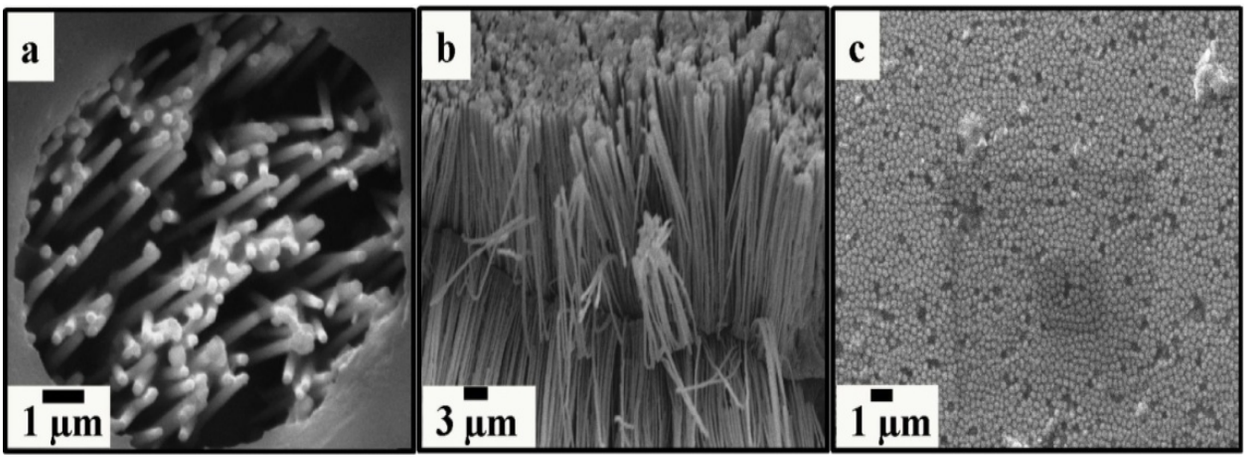

Figure 9. Scanning electron micrograph (SEM) of electrodeposited nanostructure in (a) Polycarbonate and (b) & (c) Anodic alumina.

Transmission electron microscopy

Transmission Electron Microscope (TEM) is a widely used instrument for characterizing the interior structure of materials. For TEM, the template was completely etched and rinsed several times with deionised water to clean the residual template part. Template etching is an important step of sample preparation of nanowires for TEM characterization. Cobalt nanowires were scratched from the substrate and ultrasonicated in acetone for 15 min so that the nanowires could disperse properly. Few drops of the suspension were then transferred on to a carbon coated copper grid and the microstructures were analyzed by high resolution TEM (HRTEM: Technai G20 S-Twin model) operating at 200 kV. To get the actual diameter of the nanowire, the complete dissolving of residual template from surrounding the nanowires is very important. Typical TEM results obtained are shown in Figure 10. While nanowires grown in PCTE templates typically have a tapered cross-section due to the non-uniform diameters of the pores, the AAO template-based nanowires grow in a more uniform manner.

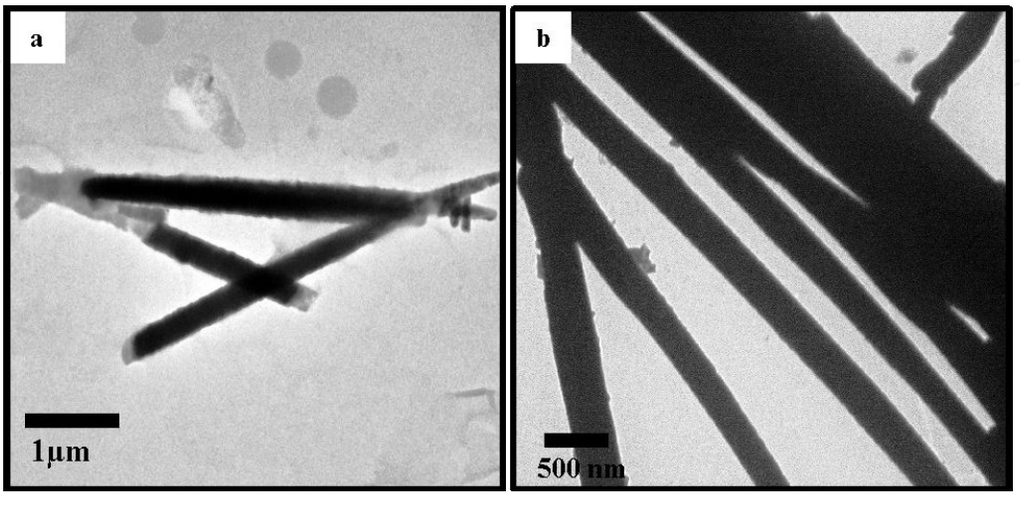

Figure 10. Transmission electron micrograph (TEM) of electrodeposited nanostructure in (a) Polycarbonate and (b) Anodic alumina.

7. Electron paramagnetic resonance

EPR/FMR measurements obtained from ferromagnetic nanowire arrays give detailed information on the size of the nanowires. The spectra can be used to calculate the interwire magnetic interactions quite accurately [31]. In Fig. 11 are shown typical spectra obtained from Co nanowire arrays. Here, both single-Co nanowire arrays and multilayered Co/Pd nanowire arrays are compared. There is clearly an angular dependence of the applied microwave field with respect to the easy axis of the nanowires, as has been studied previously [32].

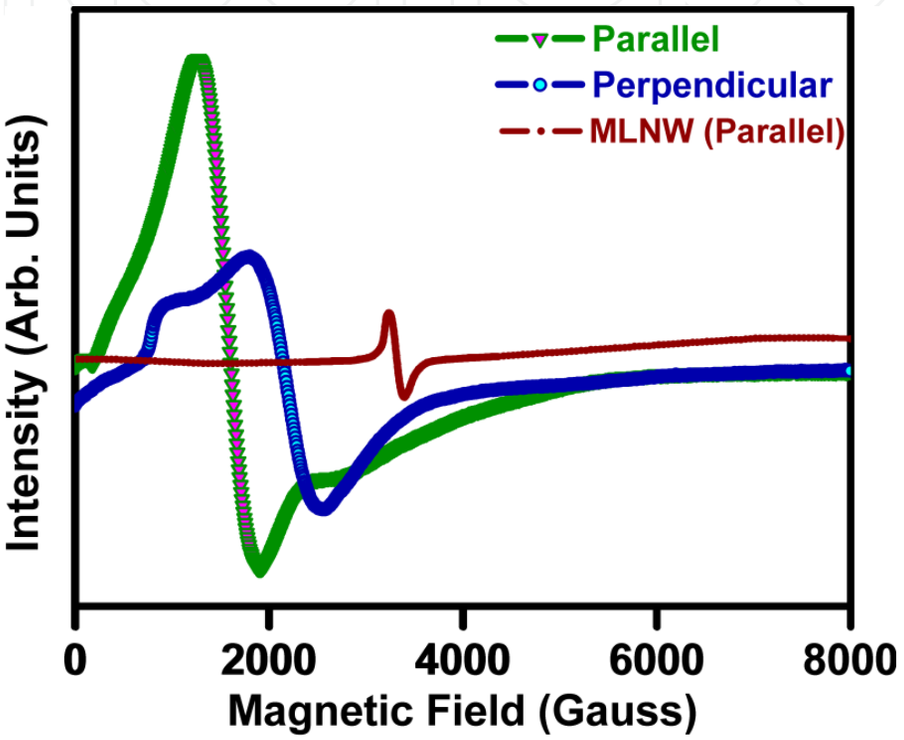

Figure 11. Electron paramagnetic resonance (EPR/FMR) spectra of single element Co nanowire arrays in parallel and perpendicular orientation at room temperature.

Fig.12 shows the FMR spectra of Co/Pd MLNW arrays for the temperature range from 90K to 290K. It is clear from the data that two different peaks in the FMR spectrum have been observed. The peak present at the ~ 3310 G is corresponding to the main peak of FMR and it is due to the quantum confinement in the nanostructures which is more in case of Co/Pd multilayered nanowires. The spin waves are confined in the magnetic nanostructure and it is found to be dominant when we reduce the third dimension (in z-direction) of the nanostructure. This main FMR peak present at all the temperature and the variation of resonance field at different temperature is very slow. As we go down to the 90K with decrease of 20K from room temperature the resonance field increases slowly. This slow variation can be explain as temperature decreases the M_s (T) increase and resultant head-to-tail alignment between FM segments increases, which further reduces the effective field as a result slow increase in the resonance field. Inset in Fig.12 shows the variation of resonance field with temperature.

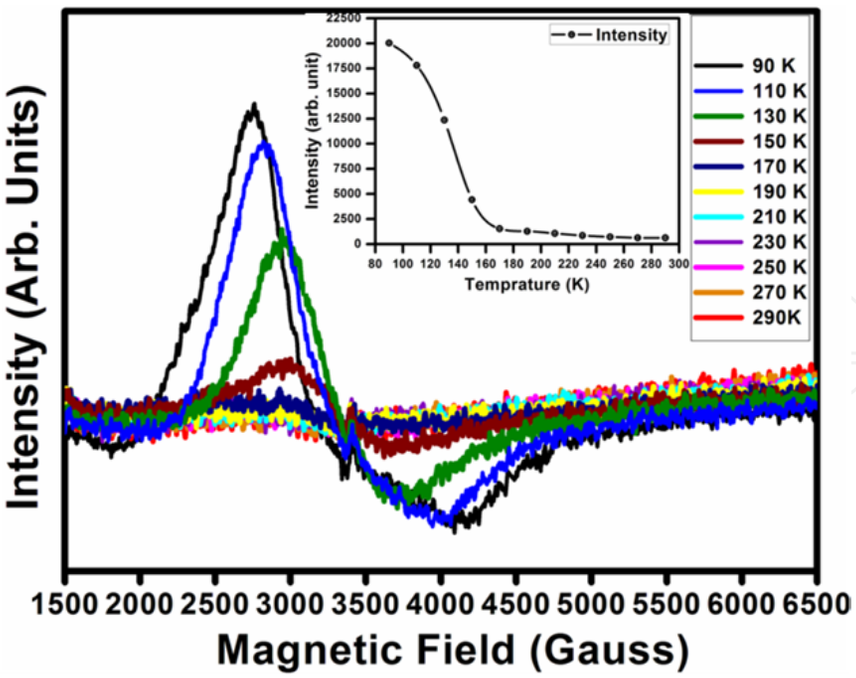

Figure 12. Electron Spin resonance (ESR/FMR) spectra of multilayered Co/Pd nanowire arrays in parallel orientation with temperature range (90K-290K). (Inset) Peak height change with temperature.

8. Microwave devices

The increasing demand for higher frequency magnetic microwave structures triggered a tremendous development in the field of magnetization dynamics over the past decade. In order to develop smaller and faster devices, a better understanding of the complex magnetization precessional dynamics, the magnetization anisotropy, and the sources of spin scattering at the nanoscale is necessary [23-25]. Magnetic data storage with its promise of non-volatility, robustness, high speed and low energy dissipation attracted long back. It has been encountered in a number of applications such as smart cards, hard drives, thin film read heads or video tapes [26-28]. Industry activities are also directed to replace semiconductor random access memories by magnet based memory devices. Logical 0 and 1 are encoded by the direction of the magnetization of a small magnetic element, such as a giant magnetoresistance (GMR) or tunneling magnetoresistance (TMR) element. For data manipulation *i.e.* reading and writing, the magnetization has to be switched between the two equilibrium positions. In order to push forward data transfer rates which are already in the GHz range, spin waves transportation mechanism has to be employed in place of current semiconductor based devices [29-32]. To this end an understanding of the dynamic motion and the mode spectrum is necessary.

On the road towards the size reduction of microwave devices, ferromagnetic nanowires embedded into porous templates have proven to be an interesting route to ferrite based materials. The main advantages of what we call ferromagnetic nanowired (FMNW) substrates are that they present a zero-field microwave absorption frequency that can be easily tuned over a large range of frequencies, as well as being low cost and fast to produce

over a large area as compared to standard ferrite devices. Conventional ferrite circulators need to be biased by a magnetic field to operate. This biasing field is generally provided by permanent magnet and in view of the volume reduction, we need to think of FMNW substrates which work at zero fields. A rigorous theory of microwave devices is very cumbersome due to ferromagnetic resonance (FMR) and spin-wave phenomena.

VNA-FMR is an important technique for the investigation of magnetization dynamics of low-dimensional magnetic structures and patterned microwave devices. Also, broadband flip-chip technique can be used to measure the material intrinsic and extrinsic properties by applying external magnetic field. In this chapter, we will demonstrate both techniques to have better understanding of ferromagnetic resonance. We propose fabrication and measurements of various non reciprocal microwave devices like band-stop filter, isolator and electromagnetic band-gap (EBG) structures using FMNW substrates using Ni and Co nanowires.

9. Conventional Ferromagnetic Resonance – Flip-chip based technique (FMR)

In the frequency domain measurements, the magnetic excitation is sinusoidal magnetic field h_{rf} and the response of the sample is detected by vector network analyzer. The magnetic field can be applied along parallel and perpendicular direction of the nanowires satisfying the FMR condition. The main components of the experimental setup are shown in Fig. 13. The VNA is connected to a coplanar waveguide (CPW) having a characteristic impedance of 50 Ω using coaxial cables and microwave connectors. For such radio frequency connections often coaxial cables with Teflon insulation and SMA connectors are employed. They are comparably low priced and offer a bandwidth of typically 18 GHz. The used cables should not have a metallic reinforcement.

Flip-chip based measurements are done to extract the material parameters, which are technologically important for data storage applications [31]. Fig. 13 shows the schematic of the set-up used for flip-chip measurements. Magnetic field is applied parallel to the nanowires and perpendicular to RF magnetic field, so that resonance condition must be satisfied.

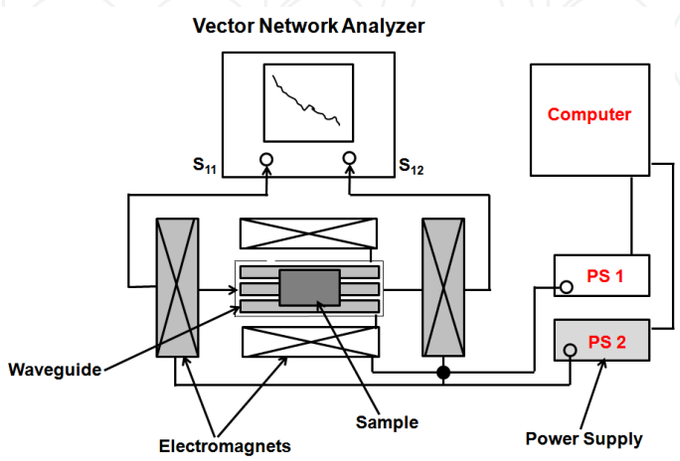

Figure 13. Schematic representation of VNA-FMR system

The transmission response of Ni NWs placed on a co-planar waveguide transmission line (Fig. 14(a)) for different static magnetic field is shown in Fig. 14(b). A small but perceptible and repeatable change was observed when the applied magnetic field was turned on/off. The change is however too small to show up in the plot of Fig. 14(b). This is partly due to masking of the shifts due to reflections from soldering and other undesirable metal deposits near the patterned transmission line and partly due to the relatively small interaction between the RF fields (largely confined to the substrate holding the CPW line) and the nanowires. It is thus expected that clearer shifts can be seen with more careful preparation and patterning of the substrate and ultimately by printing the CPW line on the nanowire template itself.

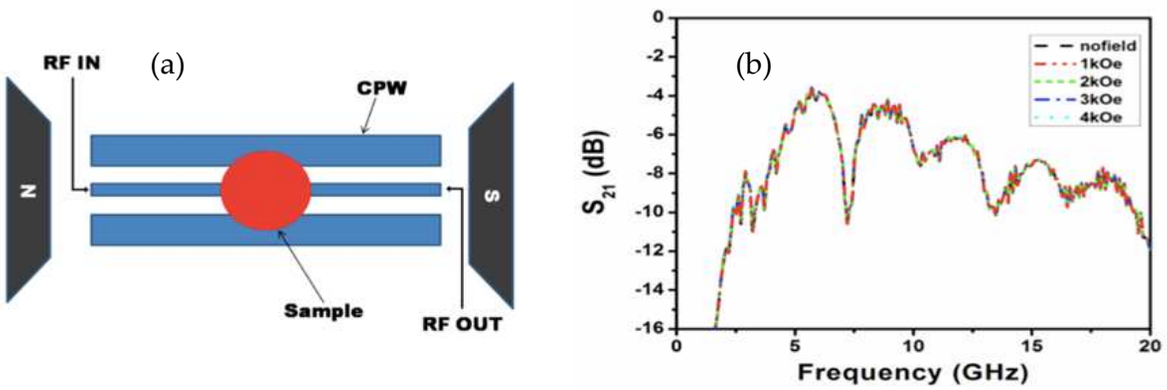

Figure 14. (a) CPW geometery for magnetic field applied along perpendicular direction (b) transmission response as a function of frequency of Ni nanowires for various applied magnetic field

10. Substrate integrated magnetic microwave devices

Newly developed techniques enable to characterize and re-arrange matter at nanometer scale. Now a day, automotive and wireless communication requires reduction in dimensions of nanodevices for yielding higher cut-off frequencies. Here, we propose integrated

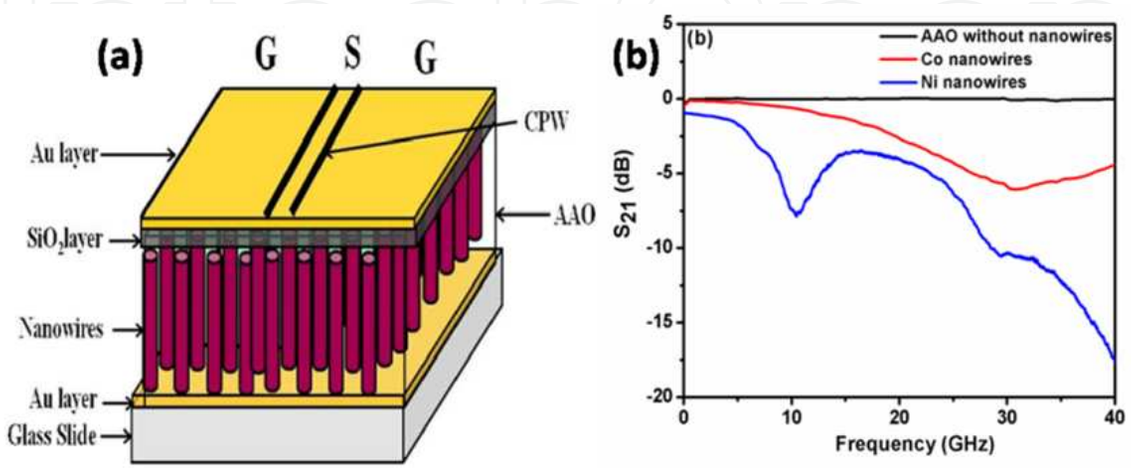

Figure 15. schematic of band stop filter (b) S-parameter of the DUT for three different samples

magnetic band-stop filter fabricated on FMNWS and studying their microwave properties like permittivity and permeability using CPW. Fig. 15(a) shows the schematic of the device under test which is a coplanar waveguide on NW substrate. The transmission coefficient of the device for three samples having bare AAO, Ni and Co NWs are shown in Fig. 15(b) at zero biasing. It is observed that by applying the magnetic field the resonance frequency shift towards higher range, so that we can tune our operating frequency of the device. We also observe that material properties also influence the Device-Under-Test (DUT).

11. Non-reciprocal devices

It is important to note that it is possible to obtain non-reciprocal structures also using nanowire-based devices. Essentially, the microwave properties like permittivity and permeability can be made to be asymmetric. This is useful to obtain non reciprocal devices such as isolators and circulators. Prototypes of such devices are presently under fabrication. Some of the proposed devices are shown in Fig. 16 below. The detailed studies of these devices are out of scope of this chapter.

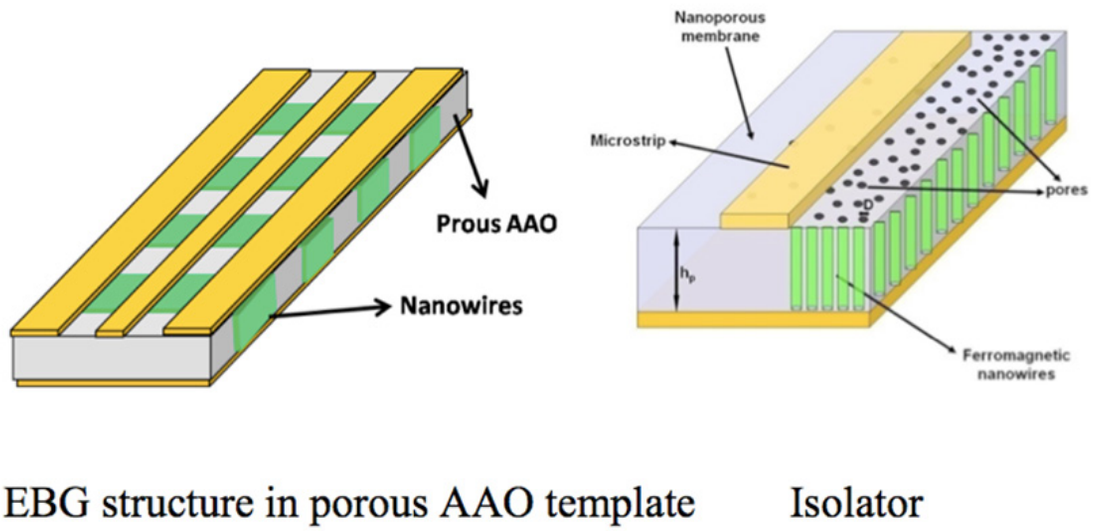

Figure 16. Possible non-reciprocal structures using nanowires.

Author details

Manish Sharma, Sachin Pathak and Monika Sharma
Indian Institute of Technology Delhi, India

12. References

[1] A. Fert and L. Piraux, "Magnetic nanowires", J. Magn. Magn. Mater. 200 (1999) 338-358.

[2] S. Shamaila, R. Sharif, S. Riaz, M. Khaleeq-ur-Rahman and X. F. Han, "Fabrication and magnetic characterization of Co_xPt_{1-x} nanowire arrays", Appl. Phys. A, 92 (2008) 687-691.

[3] Z. Z. Sun and J. Schliemann, "Fast domain wall propagation under an optimal field pulse in magnetic nanowires", Phys. Rev. Lett. 104 (2010) 037206.

[4] M. Yan, A. Kakay, S. Gliga and R. Hertel, "Beating the walker limit with massless domain walls in cylindrical nanowires", Phys. Rev. Lett. 104 (2010) 057201.

[5] C. T. Boone, J. A. Katine, M. Carey, J. R. Childress, X. Cheng and I. N. Krivorotov, "Rapid domain wall motion in permalloy nanowires excited by a spin-polarized current applied perpendicular to the nanowire", Phys. Rev. Lett. 104 (2010) 097203.

[6] B. K. Kuanr, V. Veerakumar, R. Marson, S. Mishra, R. E. Camley and Z. Celinski, "Nonreciprocal microwave devices based on magnetic nanowires", Appl. Phys. Lett. 94 (2009) 202505.

[7] M. Darques, J. De La T. Medina, L. Piraux, L. Cagnon and I. Huynen, "Microwave circulator based on ferromagnetic nanowires in alumina template", Nanotechnology 21 (2010) 145208.

[8] J. De La T. Medina, J. Spiegel, M. Darques, L. Piraux and I. Huynen, "Differential phase shift in nonreciprocal microstrip lines on magnetic nanowired substrates", Appl. Phys. Lett. 96 (2010) 072508.

[9] C. Kittel, "On the theory of ferromagnetic resonance absorption", Phys. Rev. 73 (1948) 155.

[10] C. Kittel, "Excitation of spin waves in a ferromagnet by a uniform rf field", Phys. Rev. 110 (1958) 1295-1297.

[11] L. Kraus, G. Infante, Z. Frait and M. Vazquez, "Ferromagnetic resonance in microwires and nanowires", Phys. Rev. B 83 (2011) 174438.

[12] J. De La T. Medina, L. Piraux, J. M. Olais Govea and A. Encinas, "Double ferromagnetic resonanace and configuration-dependent dipolar coupling in unsaturated arrays of bistable magnetic nanowires", Phys. Rev. B 81 (2010) 144411.

[13] A. Encinas-Oropesa, M. Demand, L. Piraux, I. Huynen and U. Ebels, "Dipolar interactions in arrays of nickel nanowires studied by ferromagnetic resonance", Phys. Rev. B 63 (2001) 104415.

[14] C. A. Ramos, M. Vazquez, K. Nielsch, K. Pirota, R. B. Rivas, R. B. Wherspohn, M. Tovar, R. D. Sanchez and U. Gosele, "FMR characterization of hexagonal arrays of Ni nanowires", J. Magn. Magn. Mater. 272-276 (2004) 1652-1653.

[15] C. A. Ramos, E. Vassallo Brigneti and M. Vazquez, "Self-organized nanowires: evidence of dipolar interactions from ferromagnetic resonance measurements", Physica B 354 (2004) 195-197.

[16] E. Beaurepaire, J. C. Merle, A. Daunois and J. Y. Bigot, "Ultrafast spin dynamics in ferromagnetic nickel", Phys. Rev. Lett. 76 (1996) 4250-4253.

[17] M. R. Freeman, and W. K. Hiebert, "Stroboscopic microscopy of magnetic dynamics", In: B. Hillebrands, K. Ounadjela (Eds.), Spin Dynamics in Confined Magnetic Structures I. Springer, Berlin, pp. 93-126.

[18] W. K. Hiebert, A. Stankiewicz, and M. R. Freeman, "Direct observation of magnetic relaxation in a small permalloy disk by time-resolved scanning Kerr microscopy", Phys. Rev. Lett. 79 (1997) 1134-1137.

[19] T. J. Silva, C. S. Lee, T. M. Crawford, and C. T. Rogers, "Inductive measurement of ultrafast magnetization dynamics in thin-film permalloy", J. Appl. Phys. 85 (1999) 7849-7862.

[20] M. M. Midzor, P. E. Wigen, D. Pelekhov, W. Chen, P. C. Hammel, and M. L. Roukes, "Imaging mechanisms of force detected FMR microscopy", J. App. Phys. 87 (2000) 6493-6495.

[21] O. Mosendz, B. Kardasz, D. S. Schmool, and B. Heinrich, "Spin dynamics at low microwave frequencies in crystalline Fe ultrathin film double layers using co-planar transmission lines", J. Magn. Magn. Mater. 300 (2006) 174-178.

[22] N. Mecking, Y. S. Gui, and C. M. Hu, "Microwave photovoltage and photoresistance effects in ferromagnetic microstrips", Phys. Rev. B 76 (2007) 224430.

[23] B. K. Kuanr, M. Buchmeier, D. E. Buergler, P. Gruenberg, R. E. Camley, and Z, Celinski, "Dynamic and static measurements on epitaxial Fe-Si-Fe", J. Vac. Sci. Technol. A 24 (2003) 1157.

[24] J. Curiale, R. D. Sanchez, C. A. Ramos, A. G. Leyva, A. Butera, "Dynamic response of magnetic nanoparticles arranged in a tubular shape", J. Magn. Magn. Mater. 320 (2008) 218-221.

[25] Can-Ming Hu, "Recent progress in spin dynamics research in Canada", La Physique Au Canada 65 (2009).

[26] X. Kou, X. Fan, R. K. Dumas, Q. Lu, Y. Zhang, H. Zhu, X. Zhang, K. Liu and J. Q. Xiao, "Magnetic effects in magnetic nanowire arrays", Adv. Mater. 23 (2011) 1393-1397.

[27] T. Schrefl, J. Fidler, D. Suss, and W. Scholz, "Hysteresis and switching dynamics of patterned magnetic elements", Phys. B 275 (2000) 55-58.

[28] X. Kou, X. Fan, H. Zhu and J. Q. Xiao, "Ferromagnetic resonance and memory effects in magnetic composite materials".

[29] K. Nagai, Y. Cao, T. Tanaka and K. Matsuyama, "Binary data coding with domain wall for spin wave based logic devices", J. Appl. Phys. 111 (2012) 07D1301-07D1304.

[30] M. Sharma, S. Pathak, S. Singh, M. Sharma and A. Basu, "Highly ordered magnetic nickel nanowires: structural properties and ferromagnetic resonance measurements", AIP Conf. Proc. 1347 (2011).

[31] O. Yalçın, et al, Ferromagnetic resonance studies of Co nanowire arrays, Journal of Magnetism and Magnetic Materials 272–276 (2004) 1684–1685.

[32] G. Kartopu, O. Yalçın, et al. Size effects and origin of easy-axis in nickel nanowire arrays, Journal of Applied Physics 109, 033909 (2011).

[33] G. Kartopu, O. Yalçın, M. Es-Souni, and A. C. Başaran, Magnetization behavior of ordered and high density Co nanowire arrays with varying aspect ratio, Journal of Applied Physics 103, 093915 (2008).